Insights into pathological mechanisms of missense mutations in C-terminal domains of von Willebrand factor causing qualitative or quantitative von Willebrand disease

Hamideh Yadegari,[1] Julia Driesen,[1] Anna Pavlova,[1] Arijit Biswas,[1] Vytautas Ivaskevicius,[1] Robert Klamroth,[2] and Johannes Oldenburg[1]

[1]Institute of Experimental Haematology and Transfusion Medicine, University Clinics Bonn; and [2]Department of Angiology and Clotting Disorders, Haemophilia Treatment Center, Vivantes Hospital Friedrichshain, Berlin, Germany

ABSTRACT

The carboxyl-terminal domains of von Willebrand factor, D4-CK, are cysteine-rich implying that they are structurally important. In this study we characterized the impact of five cysteine missense mutations residing in D4-CK domains on the conformation and biosynthesis of von Willebrand factor. These variants were identified as heterozygous in type 1 (p.Cys2619Tyr and p.Cys2676Phe), type 2A (p.Cys2085Tyr and p.Cys2327Trp) and as compound heterozygous in type 3 (p.Cys2283Arg) von Willebrand disease. Transient expression of human cell lines with wild-type or mutant von Willebrand factor constructs was performed. The mutated and wild-type recombinant von Willebrand factors were quantitatively and qualitatively assessed and compared. Storage of von Willebrand factor in pseudo-Weibel-Palade bodies was studied with confocal microscopy. The structural impact of the mutations was analyzed by homology modeling. Homozygous expressions showed that these mutations caused defects in multimerization, elongation of pseudo-Weibel-Palade bodies and secretion of von Willebrand factor. Co-expressions of wild-type von Willebrand factor and p.Cys2085Tyr, p.Cys2327Trp and p.Cys2283Arg demonstrated defective multimer assembly, suggesting a new pathological mechanism for dominant type 2A von Willebrand disease due to mutations in D4 and B domains. Structural analysis revealed that mutations p.Cys2283Arg, p.Cys2619Tyr and p.Cys2676Phe disrupted intra-domain disulfide bonds, whereas p.Cys2327Trp might affect an inter-domain disulfide bond. The p.Cys2327Trp variant is distinguished from the other mutants by an electrophoretic mobility shift of the multimer bands. The results highlight the importance of cysteine residues within the carboxyl-terminal of von Willebrand factor on structural conformation of the protein and consequently multimerization, storage, and secretion of von Willebrand factor.

Introduction

Von Willebrand factor (VWF) is a multimeric plasma glycoprotein that mediates platelet adhesion to the subendothelium after vascular injury, and also protects factor VIII in the circulation.[1,2] Deficient or defective VWF results in von Willebrand disease (VWD), a common inherited bleeding disorder. VWD is classified into three major categories. Types 1 and 3 represent partial and total quantitative deficiencies of VWF, respectively. Type 2 is due to qualitative defects of VWF, and is divided into four secondary categories.[3-5] VWD type 2A, characterized by the absence of high molecular weight (HMW) multimers and decreased platelet-dependent function, is the most common form of VWD type 2.[6,7] The loss of HMW multimers in type 2A VWD results from either mutations that impair assembly and secretion of VWF multimers or variants that increase susceptibility to proteolytic cleavage by ADAMTS13.[8-10]

VWF is synthesized in endothelial cells and megakaryocytes and stored in the Weibel-Palade bodies (WPB) and α-granules, respectively, of these cells. The pre-pro-VWF comprises a signal peptide and repeated domains arranged in the order D1-D2-D′-D3-A1-A2-A3-D4-B1-B2-B3-C1-C2-CK. Pro-VWF is assembled in the endoplasmic reticulum into dimers through disulfide bonds between CK domains, and is then transported to the trans-Golgi network. There the dimers are assembled into multimers by N-terminal disulfide bonds aligned with formation of helical tubules in nascent WPB.[11,12]

Many of the VWF domains have specific functions either in hemostasis or in forming ultralong concatamers. Although the carboxyl-terminal (C-terminal) of VWF, including D4, B and C domains, is a cysteine-rich area, which may imply structural importance, no particular function has been assigned for most of these domains.[13] The classical annotation of the C-terminal domain was recently updated by Zhou *et al.*, such that the previous B and C regions of VWF have been re-annotated as six tandem von Willebrand C (VWC) and VWC-like domains, C1-C6.[14] Additionally, it has been demonstrated that the VWF C-terminals zip up and form a structure resembling a bouquet of flowers, in which the A2, A3, and D4 domains represent the flower heads while the six VWC domains form the stem.[14,15]

 doi:10.3324/haematol.2013.084111
The online version of this article has a Supplementary Appendix.
Manuscript received on January 14, 2013. Manuscript accepted on March 20, 2013.
Correspondence: johannes.oldenburg@ukb.uni-bonn.de

In this study we analyzed five different VWF mutations, affecting cysteine amino acids in the D4, B, C2 and N- terminal of CK domains; we had described four of these mutations in one of our previous works.[16] Interestingly, these gene alterations were associated with either quantitative (types 1 and 3) or qualitative VWD (type 2A). We transiently expressed the mutations *in vitro*, and characterized their effect on multimer assembly, biogenesis of WPB and secretion. The possible structural impact of these cysteine mutations was additionally studied by homology modeling. The results of this study expand our understanding of the pathophysiological mechanisms of C-terminal domain VWF mutations, which will help to establish phenotype-genotype correlations.

Design and Methods

Patients: coagulation studies and mutation analysis

Five patients, diagnosed with VWD were included in this study. The bleeding score was calculated on the basis of a Condensed MCMDM-1 VWD questionnaire.[17] Laboratory investigations of VWF antigen (VWF:Ag), VWF ristocetin cofactor activity (VWF:RCo), factor VIII coagulant activity (FVIII:C) and VWF multimers [1.2% (w/v) and 1.6% (w/v) agarose gels] were performed as previously described.[16,18] All mutations were identified by direct sequencing of the *VWF* coding region as previously described.[16] This study was approved by the local ethics committee and informed consent was obtained from all patients. *(Online Supplementary Methods)*

Plasmid constructs

Mutations were introduced into the pMT2-VWF plasmid containing human full-length wild-type (WT) VWF cDNA using the QuickChange II XL site-directed mutagenesis kit (Stratagene, CA, USA).

Cell culture and transfection

Human embryonic kidney cell lines HEK293T and HEK293 (DSMZ, Braunschweig, Germany) were used to evaluate secretion and intracellular location of WT and mutant recombinant VWF (rVWF), respectively. Both cell lines were cultured in Dulbecco's modified Eagle's medium (DMEM) supplemented with 10% (v/v) fetal bovine serum (Life Technologies, CA, USA) at 37°C in a 5% CO_2 atmosphere.

Cells were transiently transfected with 8 μg of rVWF-WT or mutated VWF constructs using liposomal transfer (Lipofectamine 2000; Life Technologies, CA, USA). Co-transfections were performed using an equal amount of WT and mutant vectors to reproduce heterozygous states in patients. Seventy-two hours after transfection of HEK293T cells, supernatants were collected and cells were lysed for analysis of intracellular VWF.[19] *(Online Supplementary Methods)*

Quantitative and qualitative analysis of von Willebrand factor

The amount of VWF:Ag secreted into the medium and VWF:Ag present in cellular lysate were determined. Activity of secreted rVWF was assessed by binding to platelet GPIb, collagen type III (VWF:CB), and VWF:RCo. The mean values of the groups were compared with the Student's t-test. The multimers of secreted rVWF were analyzed as described above.

ADAMTS13 assay

To assess the susceptibility of mutants of VWF to proteolysis, full-length WT and mutated rVWF (6 μg/mL) were cleaved by 3 μg/mL of recombinant ADAMTS13 (R&D systems, USA) and then subjected to agarose gel electrophoresis.

Immunofluorescence analysis

Transfected HEK293 cells were stained with immunofluorescent antibodies to visualize VWF, *cis*- and *trans*-Golgi network and endoplasmic reticulum.[20] The cells were analyzed with Olympus Fluo View FV1000 or a Leica SL confocal microscope. *(Online Supplementary Methods)*

Homology modeling of von Willebrand factor C1, C5, C6 domains and molecular dynamic simulation analysis

Homology modeling for the C1, C5, and C6 domains based on recent domain annotations[14] was done using different software platforms, such as the LOMETS server [*http://zhanglab.ccmb.med.umich.edu/LOMETS/*; accessed between 01.07.2012 and 10.07.2012][21] and YASARA version 12.8.6.[22] The resulting models were further refined by a 500ps MD simulation (AMBER03 force field) in YASARA version 12.8.6.[23] The monomer models were run on the online server CLUSPRO in dimer mode [*http://cluspro.bu.edu/home.php*; accessed between 15.08.2012 and 15.10.2012].[24] The impact of the mutation on folding was calculated using the FOLDX plugin incorporated in YASARA version 12.8.6.[25] Classical molecular dynamic simulation analysis was done for the wild-type and mutant domain variants using

Table 1. Mutations and phenotypic characteristics of patients.

#	VWD type	Sex/Age (years)	Nucleotide exchange	AA exchange	Domain (original designations)	Domain (updated designations)	VWF:Ag IU/dL	VWF:RCo IU/dL	FVIII:C IU/dL	Multimer pattern	Bleeding Score (BS)	Bleeding symptoms
1	2A	M/25	c.6254G>A	p.Cys2085Tyr	D4	D4	22	13	42	Abnormal	13	1,2, 3, 5
2	3	M/51	c.6847T>C	p.Cys2283Arg	D4	C1	3	5	6	No HMW, Intermediate and LMW multimers	15	1, 2, 3, 5, 6, 10
			c.3679T>C	p.Cys1227Arg	D3							
3	2A	F/74	c.6981T>G	p.Cys2327Trp	B	C1	13	7	22	Abnormal	20	1, 2, 3, 4, 6, 8, 9
4	1	F/24	c.7856G>A	p.Cys2619Tyr	C2	C5	37	43		Normal	6	5, 7
5	1	F/18	c.8027G>T	p.Cys2676Phe	C2-CK	C6	39	30	84	Normal	3	1,7

HMW, high molecular weight; LMW, low molecular weight. The numbers listed in bleeding symptoms column represent: 1 = epistaxis, 2 = easy bruising, 3 = bleeding from minor wounds, 4 = bleeding from oral cavity, 5 = bleeding after tooth extraction, 6 = postoperative bleeding, 7 = menorrhagia, 8 = postpartum hemorrhage, 9 = muscle hematomas, 10 = CNS bleeding.

YASARA version 12.8.6 for a period of 10 nanoseconds.[26] *(Online Supplementary Methods)*

Results

Characterization of patients

Genotype, laboratory parameters, bleeding symptoms and bleeding scores of all five patients are presented in Table 1. Mutation analysis revealed six different variants (p.Cys1227Arg, p.Cys2085Tyr, p.Cys2283Arg, p.Cys2327Trp, p.Cys2619Tyr, p.Cys2676Phe) all present in the heterozygous state. In four patients the mutations were detected as single gene defects associated with type 2A VWD (patients 1 and 3) and type 1 VWD (patients 4 and 5). Two mutations p.Cys2283Arg and p.Cys1227Arg were detected in a patient with type 3 VWD (patient 2). All mutations, except p.Cys1227Arg were localized in the C-terminal end of VWF (domains D4, B, C2 and C2-CK, corresponding to the D4, C1, C5 and C6 domains up-dated by Zhou *et al.*).[14] Bleeding symptoms and the bleeding score were recorded in relation to the type of VWD.

Expression of von Willebrand factor mutations in human cell lines

To characterize the effect of the identified mutations on VWF processing, transient transfections were performed and rVWF:Ag levels were measured in both the conditioned culture media and cell lysates and expressed as a percentage of the corresponding wild-type rVWF levels. Five expression vectors corresponding to each mutation were homozygously expressed in HEK293T cells. The secretion of all mutants was severely impaired. The levels of rVWF:Ag in medium were significantly lower than those in the medium of cells expressing WT-VWF, ranging from 7% to 23% of the rVWF-WT values (Figure 1, left side). To mimic a state of heterozygosity in the patients, four mutants (p.Cys2085Tyr, p.Cys2327Trp, p.Cys2619Tyr, p.Cys2676Phe) were co-expressed with WT. The rVWF:Ag values showed reduced secretion, in the range of 45.7 to 59.5% of WT (Figure 1, right side).

Furthermore, co-expression of variants p.Cys2283Arg and p.Cys1227Arg (representing the compound heterozygous state of the type 3 VWD patient) resulted in strongly reduced secretion of VWF to 19% (Figure 1, right side).

The measurement of intracellular rVWF:Ag of all mutants showed values higher than that of the WT, indicating intracellular retention of rVWF-mutants (Figure 1).

Functional characterization of recombinant von Willebrand factor mutants

The multimer distribution of the recombinant variants demonstrated a range of structural abnormalities (Figure 2). Single transfections rVWF-p.Cys2085Tyr, p.Cys2283Arg and p.Cys2676Phe exhibited only dimers and tetramers. Multimer analysis of secreted rVWF-p.Cys2327Trp revealed a complete lack of intermediate and high molecular weight multimers, whereas rVWF-p.Cys2619Tyr showed loss of most of intermediate multimers and lack of HMWM (Figure 2A). Interestingly, variant C2327W additionally showed shift in mobility of multimer bands (Figure 2A).

Figure 2B illustrates the multimer patterns for co-expressed mutants and WT as well as for co-expression of the two mutants p.Cys2283Arg and p.Cys1227Arg, identified in the type 3 VWD patient. The co-expression of WT with mutants p.Cys2619Tyr and p.Cys2676Phe led to secretion of the full range of VWF multimers. This profile corresponds to the multimer pattern observed in the patient with type 1 VWD (Figure 2C). The multimer structure of

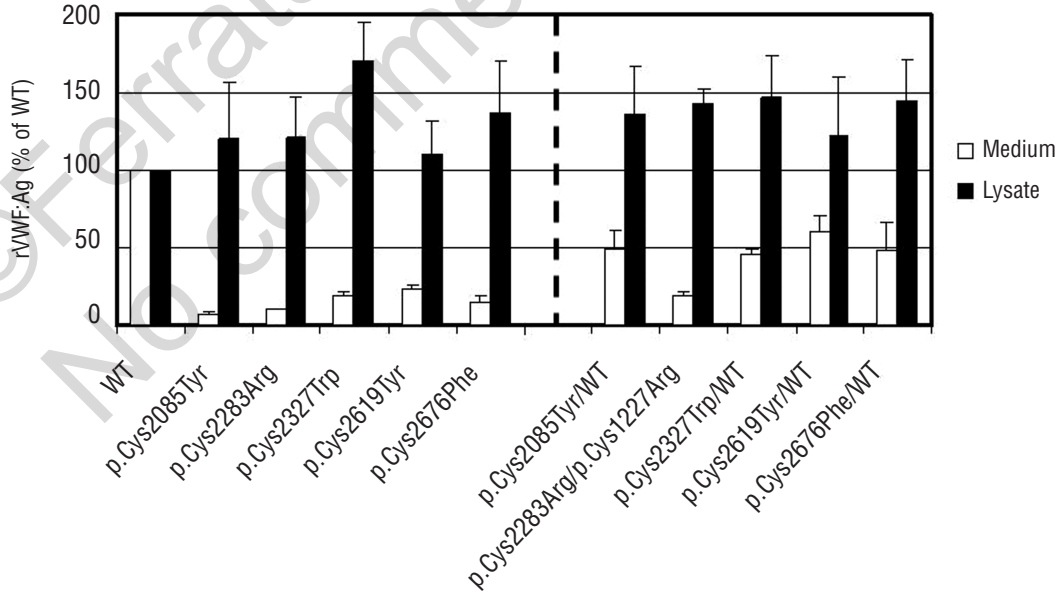

Figure 1. Recombinant VWF levels in medium and lysates. Recombinant VWF antigen levels (VWF:Ag) in medium (white bars) and lysate (black bars) are expressed as percentage relative to the amount of VWF:Ag in the medium and lysate of cells expressing WT-VWF. Each column represents the mean and standard deviations of at least three independent experiments in triplicate. Co-transfections of WT and mutant VWF cDNA were done with a 1:1 ratio.

the second group of co-expressions of p.Cys2085Tyr/WT, p.Cys2327Trp/WT and p.Cys2283Arg/WT showed a reduction of the largest multimers in secreted VWF compared with WT which correlates with the type 2A patients' phenotype. The observed reduction is so intense in co-expressions of p.Cys2085Tyr/WT that it even led to the loss of the largest multimers. The p.Cys2283Arg/p.Cys1227Arg co-expression resulted in detection of only a few low molecular weight multimers.

The functional assessment of heterozygously expressed variants is presented as ratios of VWF:RCo, GPIb binding and VWF:CB to VWF:Ag of secreted VWF (Table 2). Since the VWF levels in media of single mutant transfections were too low for reliable quantification, VWF activity assays were only performed for co-expressions of mutant/WT. Co-expressions of p.Cys2085Tyr/WT, p.Cys2283Arg/WT and p.Cys2327Trp/WT with impaired multimer structure showed decreases in ratios VWF:RCo, GPIb binding and CWF:CB to VWF:Ag compared with those of rVWF-WT ($P<0.05$), while variant p.Cys2619Tyr/WT with a normal multimer had normal binding activities, as expected. However, p.Cys2676Phe/WT revealed reduced VWF activities ($P<0.05$ *versus* wild type) in spite of normal multimers.

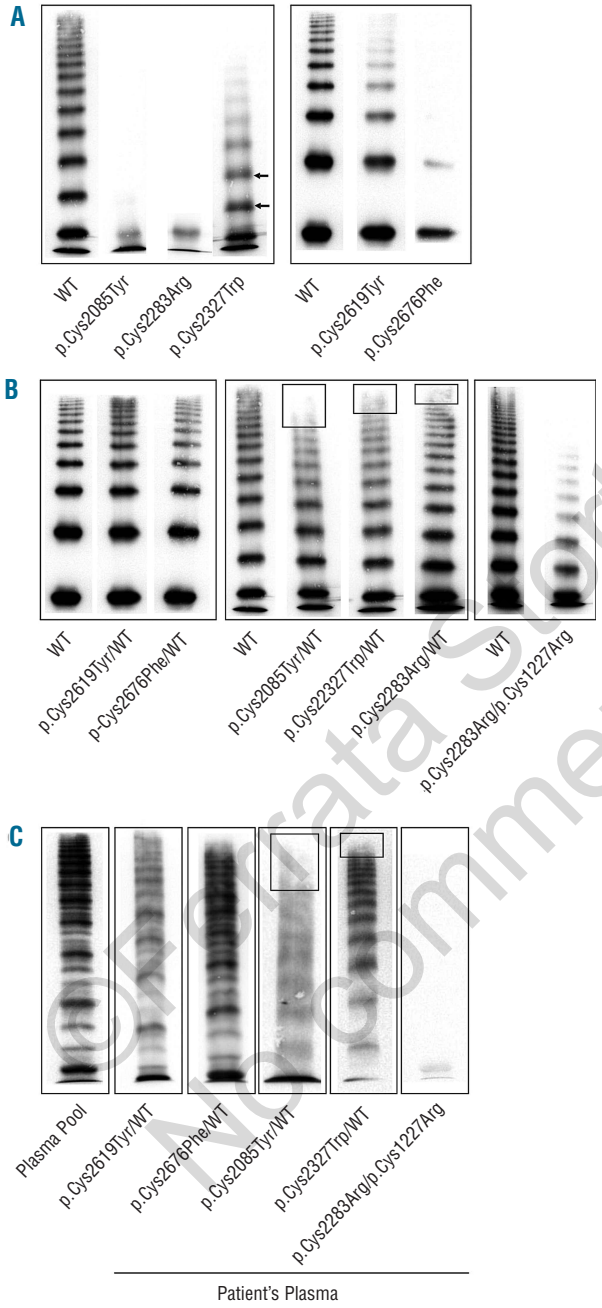

Figure 2. VWF multimeric analysis of patients and secreted rVWF after SDS-agarose gel electrophoresis. Panels (A) and (B) illustrate multimer analysis of rVWF-mutants in medium after single transfections and cotransfections, respectively, compared to rVWF-WT. Arrows indicate anodic shifts of multimeric bands observed for rVWF-p.Cys2327Trp. Boxes indicate reduction or loss of large multimers. Panel (C) represents multimer analysis of patients' plasma.

Susceptibility of variants to cleavage by ADAMTS13

We investigated whether mutants have altered susceptibility to ADAMTS13 proteolysis. Proteolytic degradation of rVWF-mutants was compared to that of the rVWF-WT. No difference in the sensitivity of the rVWF mutants to cleavage by ADAMTS13 was found (*data not shown*).

Intracellular localization

Intracellular trafficking and the impact of mutations on granule formation were analyzed after expression of mutants in HEK293 cells. HEK293 cells form pseudo-WPB granules when transfected with rVWF-WT.[8,27] Confocal microscopy showed no retention of all mutant rVWF in either the endoplasmic reticulum or in the *cis*- or *trans*-Golgi compartments (*data not shown*). Each of the VWF mutants was able to form pseudo-WPB storage granules (Figure 3, presented as small dots), although the morphology of these granules differed from the normal cigar-shaped granules formed by rVWF-WT. The majority of the pseudo-WPB granules formed by mutants were relatively shorter. We also investigated the impact of VWF variant heterozygosity on storage in pseudo-WPB granules. Upon co-transfection with rVWF-WT, the defects in the elongation of the pseudo-WPB granules caused by mutations were partially corrected (*data not shown*).

Impact of the mutations on von Willebrand factor structure

Homology modeling

The C1, C5 and C6 domains (according to Zhou *et al.*) are cysteine-rich domains characterized by multiple cysteine disulfide bonds. The domains consist of short β-strands

Table 2. Functional assays of secreted recombinant VWF proteins.

	VWF:RCo/VWF:Ag	VWF:GPIb/VWF:Ag	VWF:CB/VWF:Ag
WT	0.779±0.205	0.717±0.108	0.625±0.103
p.Cys2085Tyr/WT	0.632±0.131	0.538±0.036	0.408±0.139
p.Cys2283Arg/WT	0.496±0.129	0.581±0.068	0.543±0.131
p.Cys2327Trp/WT	0.465±0.026	0.591±0.064	0.471±0.017
p.Cys2619Tyr/WT	0.703±0.133	0.709±0.054	0.526±0.063
p.Cys2676Phe/WT	0.611±0.057	0.529±0.035	0.426±0.088

Mean and standard deviations of ratios VWF:RCo, GPIb and CB to VWF:Ag three independent co-experiments in triplicate. VWF:Ag, VWF:antigen; VWF:RCo, VWF ristocetin cofactor activity; GPIb, platelet GPIb binding; VWF:CB, collagen binding.

linked by a combination of β-turns and hairpins with the occasional short β-bulge (localized disruption of β-sheet hydrogen bonding) (C6) or α-helix (C5 & C6) (Figure 4). Only the C1 domain shows unpaired cysteines (n=4) (Figure 4); the remaining cysteines form intra-domain/intra-chain disulfide bonds.

Molecular dynamic simulation and stability prediction

The simulation of the monomeric C1, C5 and C6 domains showed high root mean square deviation (RMSD) which finally stabilized between 2-2.5A°. Comparison of trajectory RMSD for the short period of 10 ns showed differences between the mutation and the wild-type structures

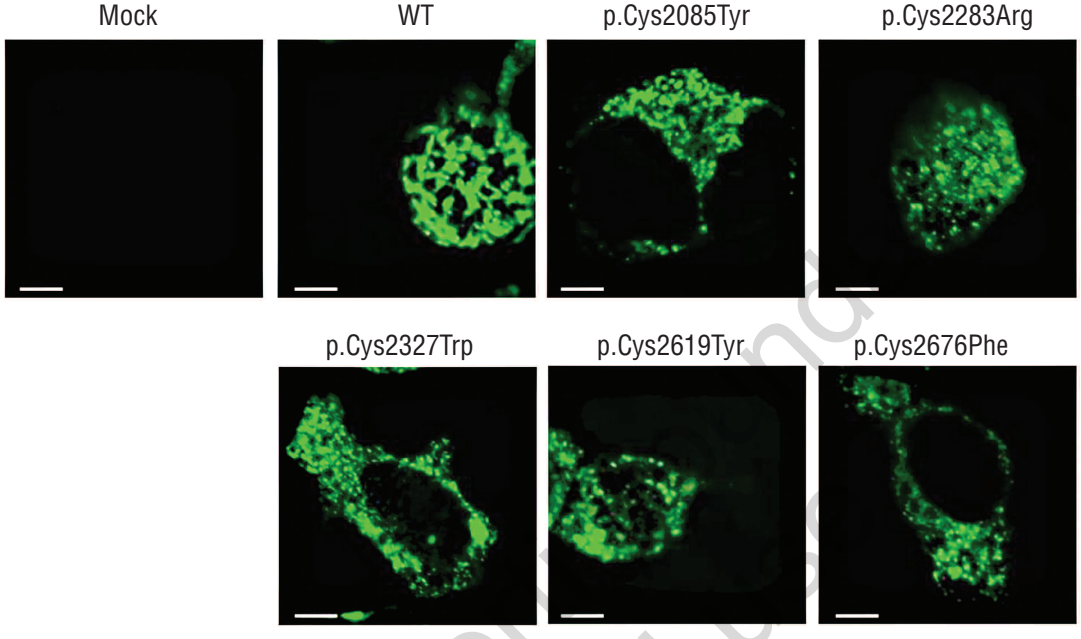

Figure 3. Intracellular storage of rVWF-WT and mutants in HEK293 cells. The pseudo-WPB granules formed after single transfections of HEK293T cells with WT and mutated constructs and mock transfected cells. Pseudo-WPB granules are shown in green (VWF staining). Pseudo-WPB granules in cells expressing rVWF-WT have a cigar-shaped appearance, while they are round and shorter in cells expressing rVWF-mutants. Scale bar = 10 μm.

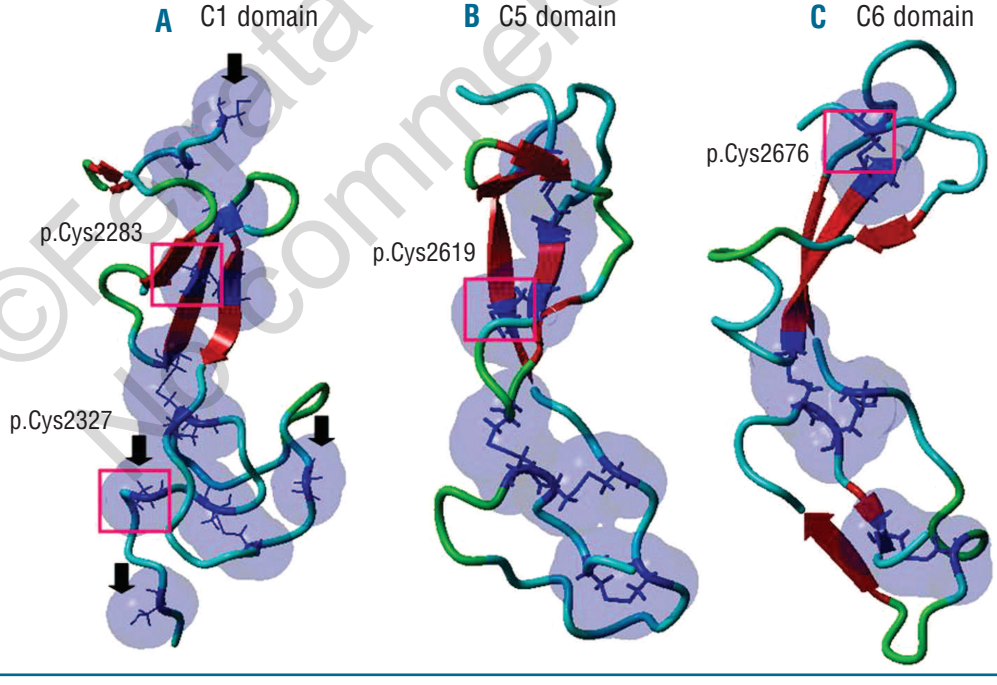

Figure 4. Homology models for C1, C5 and C6 domains. Panels (A), (B) and (C) show ribbon diagrams for the homology models of C1, C5 and C6 domains. The cysteines (unpaired and bound) are represented in stick forms. The accessible surface areas of the unpaired and bound cysteines are represented as blue spheres. The arrows in Panel A show the unpaired cysteines in domain C1. The pink boxes show the position of Cys2283 and Cys2327 in the C1 domain, Cys2619 in the C5 domain and Cys2676 in the C6 domain.

(*Online Supplementary Table S1*). Trajectory analysis for other components such as accessible surface area and the radius of gyration also showed differences between the mutations and the wild-type form (*Online Supplementary Table S1*). Folding energy calculations showed a strong impact for all the mutations except p.Cys2327Trp in the C1 domain. The p.Cys2283Arg mutation results in the replacement of a buried, conserved, disulfide-bonded cysteine residue to a polar, charged, large Arg residue which is partly surface exposed (Figure 5A). The p.Cys2327 residue was the only cysteine that is observed at the interface of the C-domain dimer models (*models not shown*). The p.Cys2327Trp

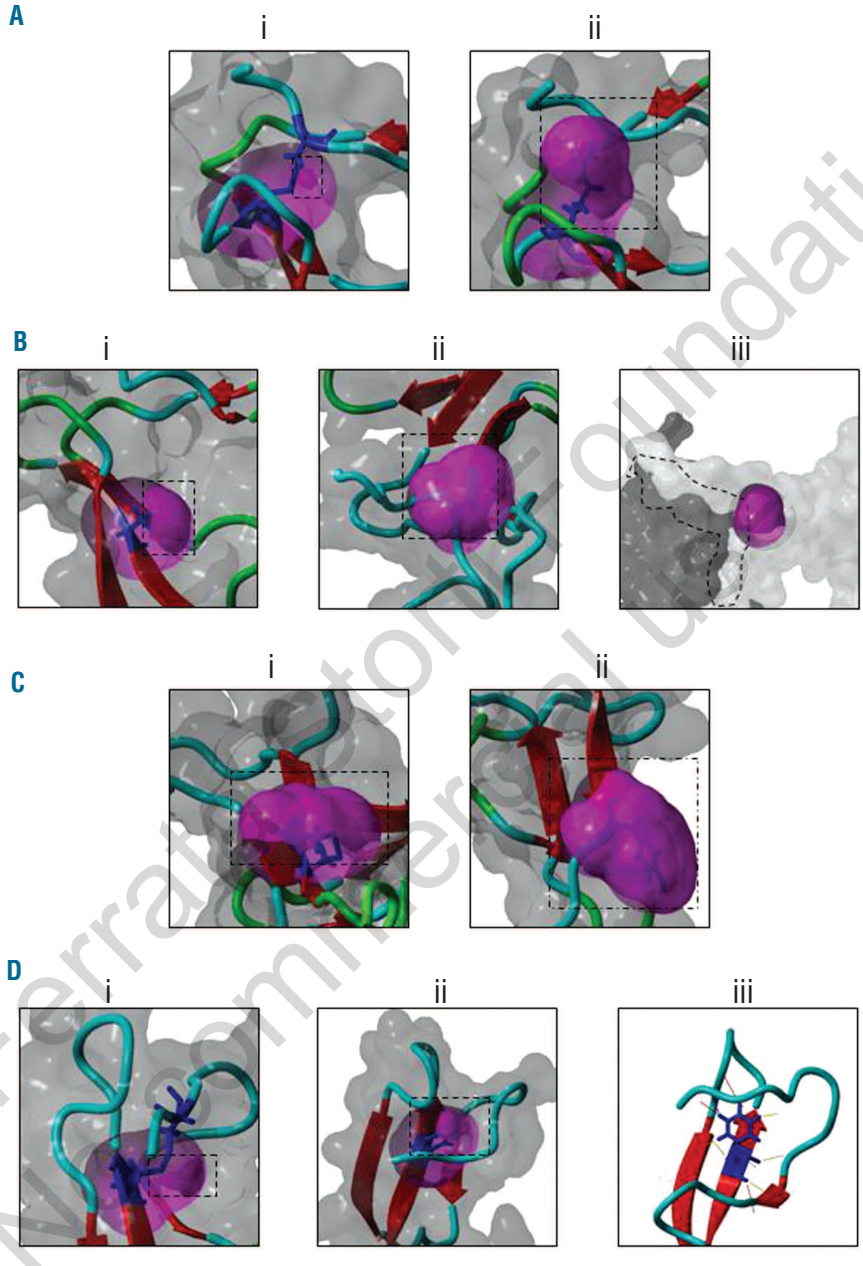

Figure 5. Close-up view of mutated and wild-type residues after molecular dynamic simulation. The representations are in surface diagrams with the backbone depicted in ribbon form. The affected residues are illustrated as blue stick representations. The surfaces of the model and affected residue are depicted in gray and magenta surface representations. The accessible surface area for the residues is highlighted by dotted rectangles and squares. Panel (A) shows the wild-type p.Cys2283 (i) and mutant p.Cys2283Arg (ii) after 10 ns of molecular dynamic simulation. The cleavage of a disulfide bond and a distinct gain in accessible surface area is noticeable for the mutant residue. Panel (B) shows the wild-type p.Cys2327 (i), mutant p.Cys2327Trp (ii) and the C1 dimer interface (iii) after 10 ns of molecular dynamic simulation. Figure (iii) emphasizes the closeness of this locus to the hypothetical interface area (the neighboring surfaces of the individual monomers are colored in separate shades of gray and the interface is marked by dotted lines). The mutant residue shows a gain in accessible surface area with most of the Trp aromatic side chain exposed to the surface. Panel (C) shows the wild-type p.Cys2619 (i) and mutant p.Cys2619Tyr (ii) in C2 domain after 10 ns of molecular dynamic simulation. The mutant residue shows the breakage of disulfide bond and a large aromatic Tyr side chain almost completely surface exposed. Panel (D) shows the wild-type p.Cys2676 in C6 domain (i), mutant p.Cys2676Phe (ii) and contact interference (iii) after 10 ns of molecular dynamic simulation. The figure (iii) shows mutated Phe residue accommodated into the protein scaffold resulting in contact problems with the neighboring residues which are shown as colored lines.

mutation was also the only cysteine residue mutation among the ones we reported which belongs to the category of unpaired cysteines (no intra-domain disulfide bond). This cysteine was partly surface exposed and also present at the C1-C1 dimer interface (in the dimer model) (Figure 5Biii) at the C-terminal end of the domain (which connects to the C2 domain). The affected cysteine in the C5 domain p.Cys2619Tyr represents the substitution of a conserved disulfide bonded cysteine with an aromatic tyrosine side chain. The disulfide bond for the p.Cys2619 residue belongs to the RHStaple category of disulfide bonds (*Online Supplementary Table S2*). The mutation p.Cys2676Phe in the C6 domain results in the replacement of a highly conserved disulfide-bonded cysteine with a large aromatic and highly hydophobic Phe side chain. During simulation the mutated Phe side chain was accommodated within the domain (Figure 5D).

Discussion

This study presents the functional characterization of five cysteine mutations occurring in the C-terminal domains of VWF. The results showed that these mutations had disruptive impacts on multimerization, storage and consequent secretion of VWF. The last two characteristics were partly corrected when the mutations were co-expressed with rVWF-WT. While the multimer structures of p.Cys2676Phe and p.Cys2619Tyr were completely corrected by co-expression with rVWF-WT, co-expressions of rVWF-WT and p.Cys2085Tyr, p.Cys2327Trp and p.Cys2283Arg showed loss or reduction of large multimers indicating a dominant negative effect of these mutations on multimerization. Concordant with our finding, previous studies have shown impaired multimerization and intracellular retention of VWF for some homozygously expressed cysteine missense mutations at the C-terminal of VWF.[28-30] Nevertheless, this study demonstrates for the first time a defect in multimer assembly by heterozygous mutations occurring in the D4 and B domains, and presents a new pathological mechanism for dominant type 2A VWD.

All mutants exhibited apparent intracellular retention. However, when the total amount of rVWF produced (the sum of VWF:Ag in medium and lysate) was calculated, all mutant rVWF constructs (except p.Cys2327Trp) demonstrated statistically significant reduced expression of rVWF compared to rVWF-WT ($P<0.05$). These data suggest that the investigated mutations might additionally lead to increased intracellular degradation or decreased synthesis. The confocal microscopy results excluded retention of mutant rVWF in the endoplasmic reticulum and *cis*- and/or *trans*-Golgi compartments. The punctuate granular pattern observed with immunofluorescent staining showed that the mutations interfere with the normal elongation of pseudo-WPB. Previous investigations found impaired formation of normal elongated pseudo-WPB granules for *in vitro* expression of variants located in propeptide, D3 and C-terminal VWF domains.[20,30,31]

Co-expressions of WT and either p.Cys2085Tyr, p.Cys2327Trp, p.Cys2619Tyr or p.Cys2676Phe mutants clearly reproduced the phenotype observed in heterozygous patients. Co-expression of p.Cys2283Arg and p.Cys1227Arg variants caused marked reduction in secretion of rVWF, suggesting that these mutations are causative for low VWF antigen in patient's plasma. It is already known that p.Cys1227 in the D3 domain participates in an intersubunit disulfide bond, critical for multimerization.[32] Our *in vitro* experiments clearly demonstrated that the p.Cys2283Arg variant also leads to defective multimer assembly in both homozygous and heterozygous states. However, the VWF antigen levels and multimer analysis of the co-expressed mutants and patients' plasma showed slight discrepancies. The presence of a few low molecular weight VWF multimers in culture medium was in contrast to the existence of only dimers in the patients' plasma. This might be explained by instability of the low molecular weight VWF multimers composed of mutant VWF monomers, and enhanced clearance of them in plasma.

Both patients with type 2A VWD showed a smeary multimer pattern without distinguishable triplet structures indicating altered susceptibility to VWF proteolysis by ADAMTS13. Since efficiency of *in vitro* proteolysis of recombinant p.Cys2085Tyr/WT and p.Cys2327Trp/WT by rADAMTS13 was not changed compared with rVWF-WT, the altered proteolysis of mutated VWF in plasma is likely not an intrinsic property of the mutations but rather the result of strong reduction of VWF:Ag levels in plasma or unequal experimental and circulatory conditions.

Molecular modeling of the cysteine disulfide bonds on the C1, C5 and C6 domains (updated domain designations) gives rise to a number of hypotheses consistent with our experimental results. Our homology models for the C domains revealed that the cysteine residues p.Cys2283, p.Cys2619 and p.Cys2676 are involved in intra-chain/intra-domain disulfide bonds (Figure 4) in C1, C5 and C6, respectively, consistent with the predicted disulfide assignment suggested by Zhou *et al.*[14] The anomalous introduction of a surface charge with the p.Cys2283Arg substitution might influence the interaction on the surface of the domain and the large Arg side chain might result in intra-domain instability. The –RH Staple configuration shown by the disulfide bonds involving p.Cys2619 residue is typical of disulfide bonds categorized as "allosteric" disulfide bonds, responsible for regulation of protein functions depending on whether they break or form.[33,34] This bond is, therefore, critical to the overall stability of the domain since the mutation p.Cys2619Tyr, in spite of breaking a disulfide bond, does not show a remarkable change in modeled surface exposure (accessible surface area and charge) during simulation (*Online Supplementary Table S2*; Figure 5C). Accommodating the large aromatic Phe side chain in the p.Cys2676Phe mutation in the C6 domain might result in intra-domain steric clashes which could damage the overall protein scaffold, and possibly decrease the protein's stability (Figure 5Diii). The p.Cys2283Arg, p.Cys2619Tyr and p.Cys2676Phe mutations may, therefore, all result in unstable domains. This is reflected by changes in the trajectory RMSD, radius of gyrations (during simulation) as well as high folding energy change values for all these mutations. The reduced levels of VWF expression in our study also indicated protein instability for all these mutations which is in agreement with the *in sillico* data. Our C1 homology model and previous reports suggest that the p.Cys2327 might be one of the unpaired cysteines participating in an inter-domain disulfide bond with the neighboring p.Cys2632 from the C2 domain.[14] The p.Cys2327Trp is also distinguished from the other

mutants in our expression analysis by an electrophoretic mobility shift for the multimer bands confirming a major conformational change in the protein. This raises the possibility that the mutation of this cysteine to the aromatic Trp residue might create a steric interference at the point of contact for the C2 domain as well as the C1 domain from the opposite monomer resulting in a conformationally altered protein. Interestingly, this mutation, unlike the other C-domain mutations, is not predicted to result in a large folding energy change suggesting that the variant may not affect protein stability in spite of the conformational change. This correlates with our *in vitro* expression results in which total expression level was similar to that of the wild-type VWF. Interestingly, Tjernberg *et al.* reported a mobility shift in multimers for substitutions at p.Cys2362 in the C2 domain which is most likely the disulfide-bond partner of p.Cys2327 in the C1 domain.[35] Although we did not perform structural modeling for the D4 domain, it was predicted that the p.Cys2085 residue in the D4 domain participates in the intrachain disulfide bond.[14] The introduction of a large Arg side chain would disrupt the disulfide bond, and might cause domain instability.

In summary, the current structural analysis showed that mutations eliminating these cysteine residues could induce misfolding of the respective domains. We speculate that such domain misfoldings might influence dimeric bouquet formation and consequently helical assembly of tubules and storage. VWF secretion could, therefore, be defective because tubular packing of VWF is a prerequisite for physiological VWF unfurling upon exocytosis.[15,36,37] Moreover, recent studies showed that dimeric bouquet formation facilitates N-terminal disulfide linkage between VWF dimers which is colinear with assembly in tubules.[12,15] Accordingly, we assume that defects in multimerization might be attributed to disruption in zipping up of misfolded C domains into dimeric bouquet structures.

In conclusion, our results indicate that the above described cysteine residues have a crucial role in precise folding of D4 and C1, C5 and C6 domains (corresponding to the originally described D4, B and C domains) required for the proper arrangement of VWF dimer bouquets and their incorporation into growing tubules in nascent WPB. This study demonstrates that these mutations disrupt storage, and secretion of VWF through a common pathological mechanism, although their eventual outcome on multimerization might differ because of sub-molecular differences in structural alterations.

Acknowledgments

This work was supported by a research grant from the "German Society of Thrombosis and Haemostasis (GTH)" to JO. The authors would like to thank Professor Schneppenheim from the University Medical Center Hamburg-Eppendorf, Hamburg, Germany for providing plasmid pMT2-VWF. We thank Peter Hambitzer, Helena Dermer and Inga Schüring for their excellent technical assistance.

Authorship and Disclosures

Information on authorship, contributions, and financial & other disclosures was provided by the authors and is available with the online version of this article at www.haematologica.org.

References

1. Lyons SE, Ginsburg D. Molecular and cellular biology of von Willebrand factor. Trends Cardiovasc Med. 1994;4(1):34-9.
2. Haberichter SL, Fahs SA, Montgomery RR. von Willebrand factor storage and multimerization: 2 independent intracellular processes. Blood. 2000;96(5):1808-15.
3. Sadler JE. Biochemistry and genetics of von Willebrand factor. Annu Rev Biochem. 1998;67:395-424.
4. James PD, Goodeve AC. von Willebrand disease. Genet Med. 2011;13(5):365-76.
5. Yadegari H, Driesen J, Hass M, Budde U, Pavlova A, Oldenburg J. Large deletions identified in patients with von Willebrand disease using multiple ligation-dependent probe amplification. J Thromb Haemost. 2011;9(5):1083-6.
6. Schneppenheim R, Budde U, Obser T, Brassard J, Mainusch K, Ruggeri ZM, et al. Expression and characterization of von Willebrand factor dimerization defects in different types of von Willebrand disease. Blood. 2001;97(7):2059-66.
7. Lillicrap D. Genotype/phenotype association in von Willebrand disease: is the glass half full or empty? J Thromb Haemost. 2009;7 (Suppl 1):65-70.
8. Jacobi PM, Gill JC, Flood VH, Jakab DA, Friedman KD, Haberichter SL. Intersection of mechanisms of type 2A VWD through defects in VWF multimerization, secretion, ADAMTS-13 susceptibility, and regulated storage. Blood. 2012;119(19):4543-53.
9. Castaman G, Federici AB, Rodeghiero F, Mannucci PM. von Willebrand disease in the year 2003: towards the complete identification of gene defects for correct diagnosis and treatment. Haematologica. 2003;88(1):94-108.
10. Hilbert L, Federici AB, Baronciani L, Dallagiovanna S, Mazurier C. A new candidate mutation, G1629R, in a patient with type 2A von Willebrand's disease: basic mechanisms and clinical implications. Haematologica. 2004;89(9):1128-33.
11. Valentijn KM, Sadler JE, Valentijn JA, Voorberg J, Eikenboom J. Functional architecture of Weibel-Palade bodies. Blood. 2011;117(19):5033-43.
12. Springer TA. Biology and physics of von Willebrand factor concatamers. J Thromb Haemost. 2011;9 (Suppl 1):130-43.
13. Schneppenheim R, Budde U. von Willebrand factor: the complex molecular genetics of a multidomain and multifunctional protein. J Thromb Haemost. 2011;9 (Suppl 1):209-15.
14. Zhou YF, Eng ET, Zhu J, Lu C, Walz T, Springer TA. Sequence and structure relationships within von Willebrand factor. Blood. 2012;120(2):449-58.
15. Zhou YF, Eng ET, Nishida N, Lu C, Walz T, Springer TA. A pH-regulated dimeric bouquet in the structure of von Willebrand factor. EMBO J. 2011;30(19):4098-111.
16. Yadegari H, Driesen J, Pavlova A, Biswas A, Hertfelder HJ, Oldenburg J. Mutation distribution in the von Willebrand factor gene related to the different von Willebrand disease (VWD) types in a cohort of VWD patients. Thromb Haemost. 2012;108(4):662-71.
17. Bowman M, Mundell G, Grabell J, Hopman WM, Rapson D, Lillicrap D, et al. Generation and validation of the Condensed MCMDM-1VWD Bleeding Questionnaire for von Willebrand disease. J Thromb Haemost. 2008;6(12):2062-6.
18. Schneppenheim R, Lenk H, Obser T, Oldenburg J, Oyen F, Schneppenheim S, et al. Recombinant expression of mutations causing von Willebrand disease type Normandy: characterization of a combined defect of factor VIII binding and multimerization. Thromb Haemost. 2004;92(1):36-41.
19. Schneppenheim R, Michiels JJ, Obser T, Oyen F, Pieconka A, Schneppenheim S, et al. A cluster of mutations in the D3 domain of von Willebrand factor correlates with a distinct subgroup of von Willebrand disease: type 2A/IIE. Blood. 2010;115(23):4894-901.
20. Wang JW, Valentijn KM, de Boer HC, Dirven RJ, van Zonneveld AJ, Koster AJ, et al. Intracellular storage and regulated secretion of von Willebrand factor in quantitative von Willebrand disease. J Biol Chem. 2011;286 (27):24180-8.
21. Wu S, Zhang Y. LOMETS: a local meta-threading-server for protein structure prediction. Nucleic Acids Res. 2007;35(10):3375-82.
22. Krieger E, Koraimann G, Vriend G. Increasing the precision of comparative models with YASARA NOVA--a self-parameterizing force field. Proteins. 2002;47 (3):393-402.
23. Davis IW, Leaver-Fay A, Chen VB, Block JN,

Kapral GJ, Wang X, et al. MolProbity: all-atom contacts and structure validation for proteins and nucleic acids. Nucleic Acids Res. 2007;35(Web Server issue):W375-83.
24. Comeau SR, Gatchell DW, Vajda S, Camacho CJ. ClusPro: an automated docking and discrimination method for the prediction of protein complexes. Bioinformatics. 2004;20(1):45-50.
25. Van Durme J, Delgado J, Stricher F, Serrano L, Schymkowitz J, Rousseau F. A graphical interface for the FoldX forcefield. Bioinformatics. 2011;27(12):1711-12.
26. Krieger E, Joo K, Lee J, Lee J, Raman S, Thompson J, et al. Improving physical realism, stereochemistry, and side-chain accuracy in homology modeling: four approaches that performed well in CASP8. Proteins. 2009;77(Suppl 9):114-22.
27. Castaman G, Giacomelli SH, Jacobi P, Obser T, Budde U, Rodeghiero F, et al. Homozygous type 2N R854W von Willebrand factor is poorly secreted and causes a severe von Willebrand disease phenotype. J Thromb Haemost. 2010;8(9):2011-6.
28. Eikenboom J, Hilbert L, Ribba AS, Hommais A, Habart D, Messenger S, et al. Expression of 14 von Willebrand factor mutations identified in patients with type 1 von Willebrand disease from the MCMDM-1VWD study. J Thromb Haemost. 2009;7(8):1304-12.
29. Wang JW, Groeneveld DJ, Cosemans G, Dirven RJ, Valentijn KM, Voorberg J, et al. Biogenesis of Weibel-Palade bodies in von Willebrand's disease variants with impaired von Willebrand factor intrachain or interchain disulfide bond formation. Haematologica. 2012;97(6):859-66.
30. Castaman G, Giacomelli SH, Jacobi PM, Obser T, Budde U, Rodeghiero F, et al. Reduced von Willebrand factor secretion is associated with loss of Weibel-Palade body formation. J Thromb Haemost. 2012;10(5):951-8.
31. Haberichter SL, Budde U, Obser T, Schneppenheim S, Wermes C, Schneppenheim R. The mutation N528S in the von Willebrand factor (VWF) propeptide causes defective multimerization and storage of VWF. Blood. 2010;115(22):4580-7.
32. Michaux G, Hewlett LJ, Messenger SL, Goodeve AC, Peake IR, Daly ME, et al. Analysis of intracellular storage and regulated secretion of 3 von Willebrand disease-causing variants of von Willebrand factor. Blood. 2003;102(7):2452-8.
33. Schmidt B, Ho L, Hogg PJ. Allosteric disulfide bonds. Biochemistry. 2006;45(24):7429-33.
34. Chen VM, Hogg PJ. Allosteric disulfide bonds in thrombosis and thrombolysis. J Thromb Haemost. 2006;4(12):2533-41.
35. Tjernberg P, Castaman G, Vos HL, Bertina RM, Eikenboom JC. Homozygous C2362F von Willebrand factor induces intracellular retention of mutant von Willebrand factor resulting in autosomal recessive severe von Willebrand disease. Br J Haematol. 2006;133(4):409-18.
36. Michaux G, Abbitt KB, Collinson LM, Haberichter SL, Norman KE, Cutler DF. The physiological function of von Willebrand's factor depends on its tubular storage in endothelial Weibel-Palade bodies. Dev Cell. 2006;10(2):223-32.
37. Huang RH, Wang Y, Roth R,Yu X, Purvis AR, Heuser JE, et al. Assembly of Weibel-Palade body-like tubules from N-terminal domains of von Willebrand factor. Proc Natl Acad Sci USA. 2008;105(2):482-7.